DALTON

Synthesis of new amido, alkoxo and η-cyclopentadienyl derivatives of molybdenum †

Xuefeng Yan, Alexander N. Chernega, Nils Metzler and Malcolm L. H. Green

Inorganic Chemistry Laboratory, South Parks Road, Oxford, UK OX1 3QR

The new compounds [Mo(η-$Me_3SiC_5H_4$)$(NMe_2)_3$], [Mo(η-$Me_3SiC_5H_4)_2H_2$], [Mo(η-C_9H_7)$(NMe_2)_3$], [Mo(η-C_5H_5)-$(S_2CNMe_2)_3$], [Mo(η-C_5H_5)(OPr^i)$(NMe_2)_2$], [Mo(η-C_5H_5)(OPr^i)$_2$(NMe$_2$)], [Mo(η-C_5H_5)(OBu^t)$(NMe_2)_2$], [Mo(η-C_5H_5)(OBu^t)$_2$(NMe$_2$)], [Mo(η-C_5H_5)(OC_6H_2Me-4-Bu$^t_2$-2,6)$(NMe_2)_2$], [Mo(η-C_5H_5)(OC_6H_3Me-6-Bu^t-2)$(NMe_2)_2$], [Mo(η-C_5H_5)(OC_6H_4Bu^t-*p*)$(NMe_2)_2$], [Mo(OR)$_4$(HNMe$_2$)$_2$] (R = *p*-MeC_6H_4* or *p*-Bu^tC_6H_4) and [Mo(OC_6H_4Me-*p*)$_4$(NMe$_2$)$_2$]* have been prepared and characterised. The asterisk indicates the crystal structure has been determined.

The chemistry of molybdenum(IV) amido derivatives is well established.[1–9] However, amidocyclopentadienyl compounds of tetravalent molybdenum have received little attention, compared to those of titanium, zirconium and hafnium.[10–16] Recently, Herrmann and co-workers[17,18] described amido derivatives of cyclopentadienyl compounds of Nb, Ta and Mo, including the preparation of [Mo(η-C_5H_5)$(NMe_2)_3$] in diethyl ether. Recently, we also described the synthesis and characterisation of the same compound[19] and in this paper we report some chemistry of this molecule.

Results and Discussion

Reactions between Mo$(NMe_2)_4$ and RH (R = C_5H_5, $Me_3SiC_5H_4$ or C_9H_7)

The compound [Mo(η-C_5H_5)$(NMe_2)_3$] **1** may be prepared in 95% yield by treatment of Mo$(NMe_2)_4$ in benzene with an excess of cyclopentadiene.[19] It is an air-sensitive, volatile oil that can be readily purified by sublimation at 25 °C (10^{-2} Torr). As shown in Scheme 1, **1** is proposed to have a η^3-cyclopentadienyl ligand.[19] We have studied the redox properties of **1**. Square-wave voltammetry studies were conducted at 25 mV pulse height and 60 Hz. The voltammogram shows three major cathodic current peaks in the potential window from +1.2 to −2.2 V *vs.* silver wire at 1.10, 0.15 and −1.73 V respectively. These indicate three reduction processes for **1**. Similarly, cyclic voltammetry measurements also show three redox couples in the same potential window. These three features can be assigned unambiguously to three consecutive one-electron-transfer processes: $Mo^{6+} \longrightarrow Mo^{5+}$ ($E^{\circ\prime} = 920$), $Mo^{5+} \longrightarrow Mo^{4+}$ ($E^{\circ\prime} = 255$) and $Mo^{4+} \longrightarrow Mo^{3+}$ ($E^{\circ\prime} = -1665$ mV). Plots of the peak current (i_{pa} or i_{pc}) against the square root of the potential scan rate ($\nu^{\frac{1}{2}}$) gave straight lines, showing that the overall electrochemical process is controlled by the mass diffusion in the bulk of the solution. The ratios of $i_{pa}:i_{pc}$ around unity indicate these couples are chemically reversible on the time-scale of the experiment. The electrochemical data are in Table 1. The rather large peak potential difference (ΔE_p) may be attributed to the poor solvating characteristics of the solvent, tetrahydrofuran (thf).[20] This has been confirmed by careful comparison with the cyclic voltammetry of ferrocene, which is well known to undergo a one-electron-transfer reaction reversibly and often serves as a model compound as well as an internal reference. Addition of acetonitrile to the thf solution of ferrocene substantially reduces the ΔE_p values, as shown both in Table 1 and Fig. 1. The electron-transfer rate constants (k_s) of the processes $Mo^{5+} \longrightarrow Mo^{4+}$ and $Mo^{4+} \longrightarrow Mo^{3+}$ were calculated and are listed in Table 1. These studies clearly show that compound **1** undergoes rapid electron-transfer processes comparable to that of ferrocene.

The compound Mo$(NMe_2)_4$ was treated with an excess of trimethylsilylcyclopentadiene, $Me_3SiC_5H_5$, for 24 h at room temperature to give the compound [Mo(η-$Me_3SiC_5H_4$)$(NMe_2)_3$] **2** as a yellow oil in 95% yield. The mass spectrum (electron impact, EI) showed the base peak at *m/z* 367 attributable to the parent cation. Accurate microanalytical results were not obtained because of high sensitivity to oxygen and moisture. The ^{1}H NMR spectrum in C_6D_6 showed two pseudo-triplets at δ 5.59 and 5.53 which were assigned to the C_5H_4 group. One singlet at δ 2.97 was assigned to NMe$_2$ and another at δ 0.09 to Me$_3$Si. The ^{13}C-{^{1}H} NMR spectrum in C_6D_6 supported the ^{1}H NMR assignments. By analogy with compound **1**,[19] we propose that **2** has a η^3-cyclopentadienyl ring. The analytical, mass and NMR data for **2** and all the other new compounds described below are given in Table 2.

Treatment of Mo$(NMe_2)_4$ with an excess of $Me_3SiC_5H_5$ in refluxing benzene for 17 h gave the bent metallocene [Mo-(η-$Me_3SiC_5H_4)_2H_2$] **3** which, after passing a toluene solution through a short Al_2O_3 column, was isolated as a dark green solid. The FAB mass spectrum showed the presence of the parent cation minus two H ($M^+ - 2$H), which corresponds to the fragment Mo(η-$Me_3SiC_5H_4)_2$.

Treatment of Mo$(NMe_2)_4$ with indene for 5 d gave a dark orange semi-solid [Mo(η-C_9H_7)$(NMe_2)_3$] **4**. The compound decomposed during sublimation at 60 °C (10^{-2} Torr), but could be purified from the starting material Mo$(NMe_2)_4$ which slowly sublimed away at room temperature. The ^{1}H NMR spectrum in C_6D_6 showed two multiplets at δ 7.23 (2 H) and 6.68 (2 H) assignable to H_c and H_d, a triplet at δ 5.67 assignable to H_a, a doublet at δ 4.42 assignable to H_b and a singlet at δ 2.89 assignable to the NMe$_2$ groups. The ^{13}C-{^{1}H} NMR spectrum is consistent with the proposed structure.

Reactions of [Mo(η-C_5H_5)$(NMe_2)_3$] 1

Insertion of CS$_2$. Treatment of compound **1** with an excess of CS$_2$ in benzene to give reddish microcrystals of [Mo(η-C_5H_5)-$(S_2CNMe_2)_3$] **5**. The FAB mass spectrum shows the base peak at *m/z* 523 attributable to the parent cation and fragments at *m/z* 458 and 403 corresponding to [$M^+ - C_5H_5$] and [$M^+ - S_2$-CNMe$_2$] respectively. Compound **5** is fluxional on the NMR time-scale. At −40 °C there are six different signals for the methyl group (^{1}H and ^{13}C-{^{1}H}). At room temperature, however,

---

† *Non-SI units employed*: Torr ≈ 133 Pa; $\mu_B \approx 9.27 \times 10^{-24}$ J T^{-1}.

Table 1 Electrochemical data for $[Mo(\eta^3-C_5H_5)(NMe_2)_3]$ **1**

	$[Mo(C_5H_5)(NMe_2)_3]$ in thf			Ferrocene	
	$Mo^{6+/5+}$	$Mo^{5+/4+}$	$Mo^{4+/3+}$	$Fe^{3+/2+}$ (thf)	$Fe^{3+/2+}$ (thf + MeCN)[b]
$E^{\circ\prime\, a}$/mV	920	255	−1665	265	215
ΔE_p/mV (50 mV s^{-1})		208	296	240	110
ΔE_p/mV (100 mV s^{-1})	640	250	260	294	116
ΔE_p/mV (500 mV s^{-1})		376	410	494	180
$k_s{}^c$/cm s^{-1}		2.1	2.3	3.3	2.7

[a] All the potentials quoted are against a silver-wire reference electrode; $E^{\circ\prime}$ is taken as the mean of the cathodic and anodic peak potentials. $i_{pa}:i_{pc} = 1:1$. [b] The composition of the mixed solvent was 80% thf + 20% MeCN. [c] Calculated *via* $i_{pc} = 0.227nFACk_s \exp[(-\alpha nF/RT)(E_{pc} - E^{\circ\prime})]$, where *A* is the electrode area, *C* the molar concentration of the compound in solution, α the charge-transfer coefficient and all the other parameters have their usual electrochemical significance.

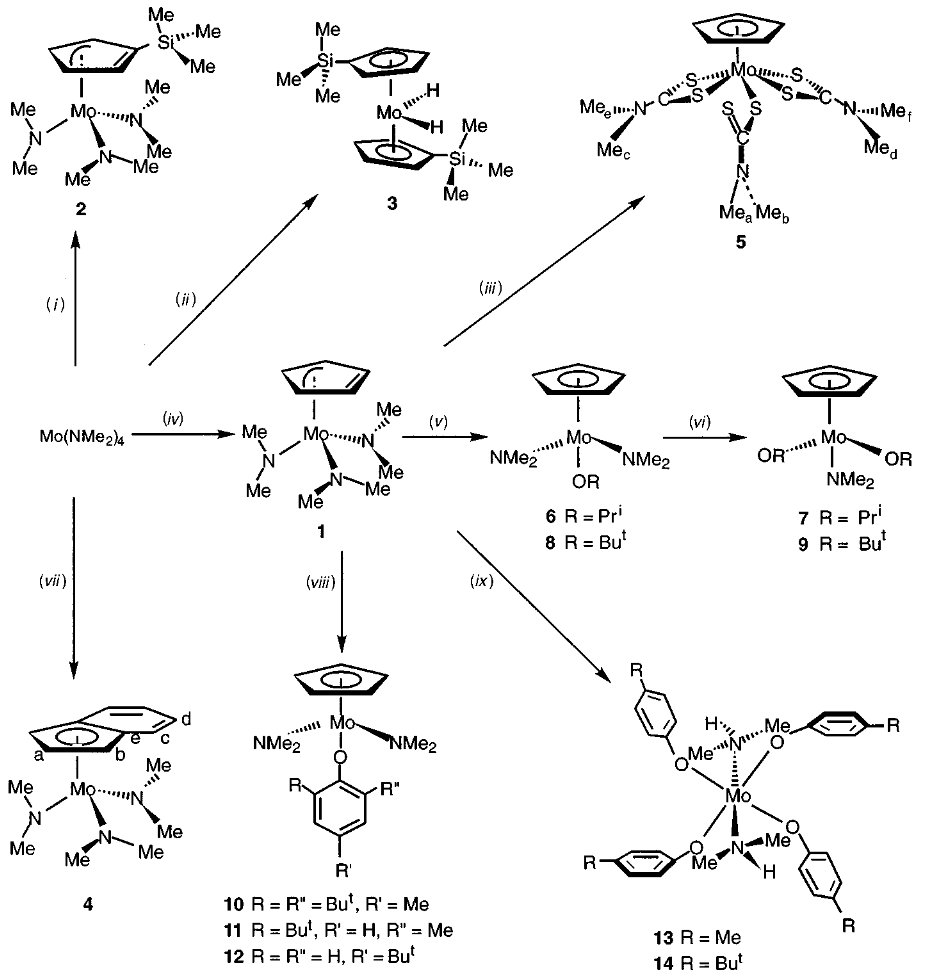

Scheme 1 (*i*) $Me_3SiC_5H_5$ (3 equivalents) in benzene at room temperature (r.t.) for 24 h, yield 95%; (*ii*) $Me_3SiC_5H_5$ excess in benzene, reflux for 17 h; (*iii*) CS_2 in benzene, reflux 2 h, 45%; (*iv*) cyclopentadiene (5 equivalents) in benzene at r.t. for 2 h, 95%; (*v*) ROH (1 equivalent) (R = Pr^i or Bu^t) in pentane at 0 °C for 30 min; (*vi*) ROH (1 equivalent) (R = Pr^i or Bu^t) in pentane at 0 °C for 30 min; (*vii*) indene (10 equivalents) at r.t. for 5 d, 50%; (*viii*) 2-R″-4′-R′-6-RC_6H_2OH in pentane; (*ix*) ROH in pentane at r.t. (R = Me or Bu^t)

four of the methyl signals in the ^1H NMR spectrum readily collapse into two signals, whereas there are still six signals in the ^{13}C-{^1H} NMR spectrum. This situation is clearly demonstrated by the indirect detection ^1H–^{13}C heteronuclear single quantum correlation (HSQC) spectrum (see Fig. 2). At 60 °C the third pair of methyl signals in the ^1H NMR spectrum also coalesce. The variable-temperature ^1H NMR spectra of $[Mo(\eta-C_5H_5)(S_2CNMe_2)_3]$ are shown in Fig. 3. The ^{13}C-{^1H} NMR spectrum also shows three resonances assignable to three CN groups.

The infrared spectrum of compound **5** shows two strong bands at 1525 and 1391 cm^{-1}, which lie intermediate in energy between the stretching frequencies of double C=N bonds (1620–1650 cm^{-1}) and single C–N bonds (1250–1350 cm^{-1}),[21] indicating partial double-bond character of the CN bonds. The band at 1525 cm^{-1} is typical for the ν(CN) stretching of molybdenum dithiocarbamates when the ligand is bidentate.[21–23] That at 1391 cm^{-1} suggests the presence of a dithiocarbamate ligand which has more single C–N bond character and therefore is adopting monodentate co-ordination. We propose that **5** has two bidentate and one monodentate thiocarbamate groups. The low-temperature (−40 °C) spectrum corresponds to slow-exchange conditions and a structure which accounts for the six bands assignable to methyl groups is shown in Scheme 1. On warming, rotation along the C–N bond in the monodentate S_2CNMe_2 group and the exchange of structures between mono- and bi-dentate ligands could cause the three pairs of methyl groups a and b, c and d, e and f to coalesce, as observed in the ^1H NMR spectrum at 60 °C. Crystals of **5** were grown by slow diffusion of pentane into CH_2Cl_2 solutions but were twinned.

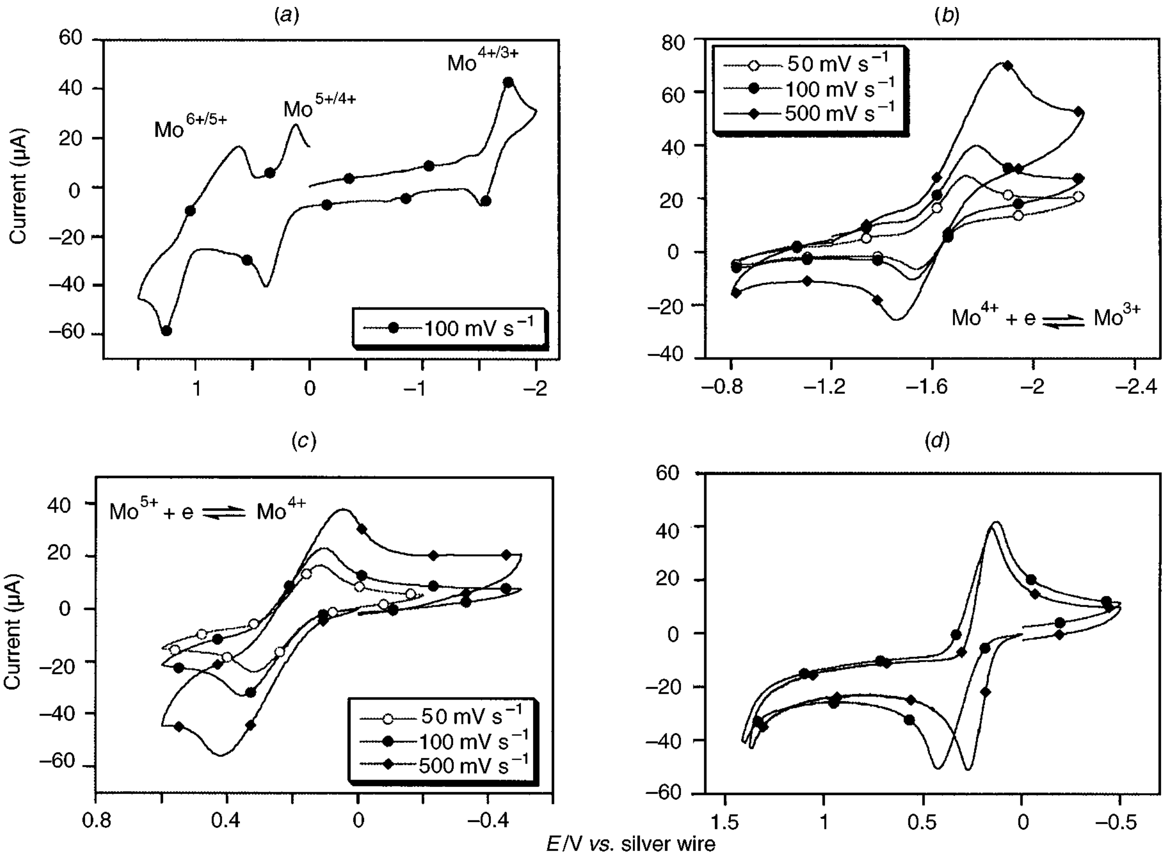

Fig. 1 Cyclic voltammograms (a)–(c) of $[Mo(\eta\text{-}C_5H_5)(NMe_2)_3]$ **1** in thf and (d) ferrocene in thf (●) and thf–MeCN (◆) (both at 100 mV s^{-1})

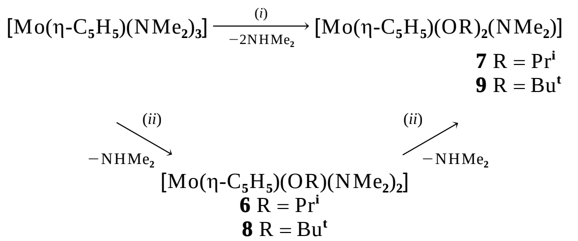

$$\begin{tikzcd}[Mo(\eta\text{-}C_5H_5)(NMe_2)_3] \arrow[r, "(i)", "-2NHMe_2"'] \arrow[dr, "(ii)", "-NHMe_2"'] & {[Mo(\eta\text{-}C_5H_5)(OR)_2(NMe_2)]\ \mathbf{7}\ R = Pr^i,\ \mathbf{9}\ R = Bu^t} \\ & {[Mo(\eta\text{-}C_5H_5)(OR)(NMe_2)_2]\ \mathbf{6}\ R = Pr^i,\ \mathbf{8}\ R = Bu^t} \arrow[u, "(ii)"', "-NHMe_2"]\end{tikzcd}$$

Scheme 2 (i) 2ROH; (ii) ROH

With alcohols. We have investigated the reactions between $[Mo(\eta\text{-}C_5H_5)(NMe_2)_3]$ and different alcohols and phenols. The reactions with Pr^iOH and Bu^tOH are summarised in Scheme 2. Treatment of **1** with 1 or 2 equivalents of Pr^iOH gave the isopropoxo derivatives $[Mo(\eta\text{-}C_5H_5)(OPr^i)(NMe_2)_2]$ **6** and $[Mo(\eta\text{-}C_5H_5)(OPr^i)_2(NMe_2)]$ **7** respectively, in essentially quantitative yields. Both compounds **6** and **7** are thermally unstable at room temperature and could only be characterised spectroscopically. The ^{13}C NMR spectra could not be obtained in the usual manner due to rapid decomposition of the sample. They were instead obtained through an indirect detection *via* ^1H–^{13}C HSQC experiments using z gradients for quick data collection (C_6D_6, the experiment time was 15 min). Compounds **6** and **7** were found to have very different chemical shifts. In order to compare their NMR spectra under identical conditions, a reaction of $[Mo(\eta\text{-}C_5H_5)(NMe_2)_3]$ **1** with 1.5 equivalents Pr^iOH was made which gave **6** and **7** in *ca.* 1:1 ratio. The ^1H and ^1H–^{13}C HSQC NMR spectra of the mixture are shown in Fig. 4 and the ^1H and ^{13}C NMR chemical shifts for **6** and **7** are listed in Table 2, where they are compared with those of Pr^iOH. The chemical shifts of the proton and carbon atoms for **6** are very similar to those of Pr^iOH. However for **7** the NMR signals of the methine proton and carbon are shifted downfield. At low temperature (−70 °C) the peaks of the ^1H NMR spectrum are sharp and have quite normal chemical shifts. However, at 70 °C C_5H_5 and $OCH(CH_3)_2$ have very unusual low-field chemical shifts and $N(CH_3)_2$ group has an unusually high-field chemical shift. The dependences of the ^1H NMR chemical shifts of compound **7** on temperature are shown in Fig. 5. We propose that the NMR behaviour can arise from the presence of an equilibrium between a diamagnetic ground state and a thermally populated electronically excited triplet state. The population of the high-spin state must be very low, even at the highest temperature of the experiment, as the observed average shifts are much smaller than normal paramagnetic shifts. The temperature dependence of these shifts does not obey the Curie law.

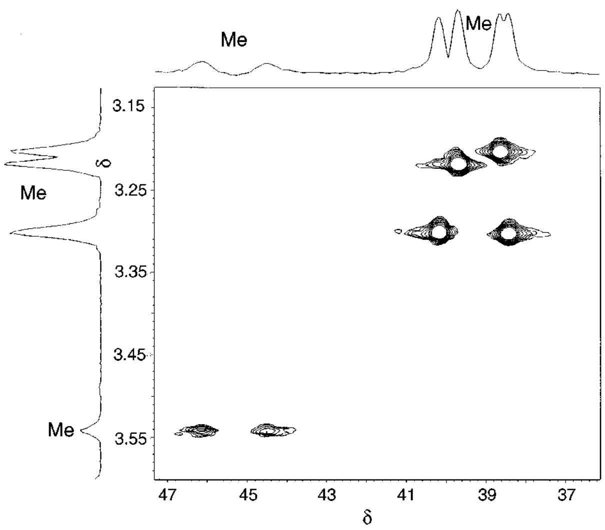

Fig. 2 The ^1H–^{13}C HSQC NMR spectra of $[Mo(\eta\text{-}C_5H_5)(S_2CNMe_2)_3]$ **5** in $CDCl_3$ at r.t.

Treatment of compound **1** with 1 or 2 equivalents of Bu^tOH gave the compounds $[Mo(\eta\text{-}C_5H_5)(OBu^t)(NMe_2)_2]$ **8** and $[Mo(\eta\text{-}C_5H_5)(OBu^t)_2(NMe_2)]$ **9**, respectively. Although these

Table 2 Characterising data for compounds **2–14**

Compound[a]	NMR data[b]
2 [Mo(η-Me$_3$SiC$_5$H$_4$)(NMe$_2$)$_3$] Green oil EI mass spectrum: *m/z* 367 (M^+), 323 ($M^+ -$ NMe$_2$), 279 ($M^+ -$ 2NMe$_2$)	^{1}H:[c] 5.59 (2 H, pseudo-t, $J_{\mathrm{HH}} = 2$, C$_5$H$_4$), 5.53 (2 H, pseudo-t, $J_{\mathrm{HH}} = 2$, C$_5$H$_4$), 2.97 (18 H, s, CH$_3$), 0.09 [9 H, s, Si(CH$_3$)$_3$] ^{13}C-{^{1}H}:[c] 107.26 (s, C$_5$H$_4$), 102.40 (s, C$_5$H$_4$, C$_{ipso}$), 99.94 (s, C$_5$H$_4$), 58.51 [s, N(CH$_3$)$_2$], 0.14 [s, Si(CH$_3$)$_3$]
3 [Mo(η-Me$_3$SiC$_5$H$_4$)$_2$H$_2$] Dark green solid C, 51.35 (51.6); H, 8.05 (7.6) FAB mass spectrum: *m/z* 372 ($M^+ -$ 2H) IR (Nujol mull): 1828m [ν(Mo–H)]	^{1}H:[c] 4.57 (4 H, pseudo-t, $J_{\mathrm{HH}} = 2$, C$_5$H$_4$), 4.27 (4 H, pseudo-t, $J_{\mathrm{HH}} = 2$, C$_5$H$_4$), 0.17 [18 H, s, Si(CH$_3$)$_3$], −8.93 (2 H, s) ^{13}C-{^{1}H}:[c] 81.2 (s, C$_5$H$_4$), 80.2 (s, C$_5$H$_4$, C$_{ipso}$), 78.9 (s, C$_5$H$_4$), 0.1 [s, Si(CH$_3$)$_3$]
4 [Mo(η-C$_9$H$_7$)(NMe$_2$)$_3$] Orange-brown thick oil C, 48.9 (52.5);[d] H, 7.3 (7.35); N, 12.05 (12.25)	^{1}H:[c] 7.23 (2 H, m, H$_c$), 6.68 (2 H, m, H$_d$), 5.67 (1 H, t, $J_{\mathrm{HH}} = 3$, H$_a$), 4.42 (2 H, d, $J_{\mathrm{HH}} = 3$, H$_b$), 2.89 (18 H, s, CH$_3$) ^{13}C-{^{1}H}:[c] 128.20 (s, C$_9$H$_7$), 124.01 (s, C$_9$H$_7$), 123.21 (s, C$_9$H$_7$), 103.37 (s, C$_9$H$_7$), 80.02 (s, C$_9$H$_7$), 54.98 (s, CH$_3$)
5 [Mo(η-C$_5$H$_5$)(S$_2$CNMe$_2$)$_3$] Red-purple powder C, 32.3 (32.25); H, 4.3 (4.45); N, 8.05 (8.05) FAB mass spectrum: *m/z* 523 (M^+), 458 ($M^+ -$ C$_5$H$_5$), 403 ($M^+ -$ S$_2$CNMe$_2$)	^{1}H (CDCl$_3$, 25 °C): 5.25 (5 H, s, C$_5$H$_5$), 3.54 (6 H, s), 3.31 (6 H, s), 3.22 (3 H, s), 3.21 [3 H, s, all N(CH$_3$)$_2$] ^{13}C-{^{1}H} (CDCl$_3$): 216.2, 208.9, 200.0 (s, all S$_2$CN), 99.6 (s, C$_5$H$_5$), 46.1 (br), 44.5 (br), 39.7, 39.2, 38.2, 38.0 [s, all N(CH$_3$)$_2$]
6 [Mo(η-C$_5$H$_5$)(OPr^i)(NMe$_2$)$_2$][e] Green oil EI mass spectrum: *m/z* 310 (M^+), 267 ($M^+ -$ Pr^i), 223 [Mo(C$_5$H$_5$)O(NMe$_2$)], 179 [Mo(C$_5$H$_5$)O]	^{1}H (500 MHz):[c] 5.22 (5 H, s, C$_5$H$_5$), 3.83 [1 H, spt, $J_{\mathrm{HH}} = 7.5$, C*H*(CH$_3$)$_2$], 3.04 [12 H, s, N(CH$_3$)$_2$], 1.17 [6 H, d, $J_{\mathrm{HH}} = 7.5$, CH(C*H*$_3$)$_2$] ^{13}C-{^{1}H} (125.7 MHz):[c] 98.9 (s, C$_5$H$_5$), 78.1 [s, *C*H(CH$_3$)$_2$], 61.9 [N(CH$_3$)$_2$], 26.2 [CH(*C*H$_3$)$_2$] For Pr^{i}OH (CDCl$_3$), ^{1}H: 4.03 [1 H, spt, C*H*(CH$_3$)$_2$], 1.21 [6 H, d, CH(C*H*$_3$)$_2$] ^{13}C-{^{1}H}: 64.2 (CH), 25.3 (CH$_3$)
7 [Mo(η-C$_5$H$_5$)(OPr^i)$_2$(NMe$_2$)][e] Green oil	^{1}H (500 MHz):[c] 6.51 (5 H, s, C$_5$H$_5$), 5.63 [2 H, spt, C*H*(CH$_3$)$_2$], 1.46 [6 H, s, N(CH$_3$)$_2$], 1.42 [6 H, d, $J_{\mathrm{HH}} = 7.5$, CH(C*H*$_3$)$_2$], 1.26 [6 H, d, $J_{\mathrm{HH}} = 7.5$, CH(C*H*$_3$)$_2$] ^{13}C-{^{1}H} (125.7 MHz):[c] 119.9 [*C*H(CH$_3$)$_2$], 102.2 (C$_5$H$_5$), 109.8 [N(CH$_3$)$_2$], 29.9 [CH(*C*H$_3$)$_2$], 28.1 [CH(*C*H$_3$)$_2$]
8 [Mo(η-C$_5$H$_5$)(OBu^t)(NMe$_2$)$_2$][e] Green oil EI mass spectrum: *m/z* 324 (M^+), 267 ($M^+ -$ Bu^t), 223 [Mo(C$_5$H$_5$)O(NMe$_2$)], 179 [Mo(C$_5$H$_5$)O]	^{1}H:[c] 5.21 (5 H, s, C$_5$H$_5$), 3.14 [12 H, s, N(CH$_3$)$_2$], 1.24 [9 H, s, C(CH$_3$)$_3$] ^{13}C-{^{1}H}:[c] 98.5 (s, C$_5$H$_5$), 78.8 [s, *C*(CH$_3$)$_3$], 62.4 [s, N(CH$_3$)$_2$], 33.0 [s, C(*C*H$_3$)$_3$] For Bu^{t}OH (CDCl$_3$), ^{1}H: 1.28 [9 H, s, C(C*H*$_3$)$_3$] ^{13}C-{^{1}H}: 69.1 [*C*(CH$_3$)$_3$], 31.2 [C(*C*H$_3$)$_3$]
9 [Mo(η-C$_5$H$_5$)(OBu^t)$_2$(NMe$_2$)][e] Green oil EI mass spectrum: *m/z* 353 (M^+), 296 ($M^+ -$ Bu^t), 223 [Mo(C$_5$H$_5$)O(NMe$_2$)], 179 [Mo(C$_5$H$_5$)O]	^{1}H:[c] 5.94 (5 H, s, C$_5$H$_5$), 1.92 [6 H, s, N(CH$_3$)$_2$], 1.31 [18 H, s, C(CH$_3$)$_3$] ^{13}C-{^{1}H}:[c] 102.4 (s, C$_5$H$_5$), 104.2 [s, *C*(CH$_3$)$_3$], 105.3 [br, N(CH$_3$)$_2$], 35.3 [s, C(*C*H$_3$)$_3$]
10 [Mo(η-C$_5$H$_5$)(OC$_6$H$_2$Me-4-Bu$^t{}_2$-2,6)(NMe$_2$)$_2$][e] Green solid	^{1}H:[c] 7.10 (2 H, s, C$_6$H$_2$), 5.28 (5 H, s, C$_5$H$_5$), 3.30 [12 H, s, N(CH$_3$)$_2$], 2.31 (3 H, s, CH$_3$), 1.36 [18 H, s, C(CH$_3$)$_3$]
11 [Mo(η-C$_5$H$_5$)(OC$_6$H$_3$Me-6-Bu^t-2)(NMe$_2$)$_2$][e] Green-brown oil	^{1}H:[c] 7.33 (1 H, d, $J_{\mathrm{HH}} = 7.5$, C$_6$H$_3$), 7.22 (1 H, d, $J_{\mathrm{HH}} = 7.5$, C$_6$H$_3$), 6.72 (1 H, pseudo-t, $J_{\mathrm{HH}} = 7.5$, C$_6$H$_3$), 5.49 (5 H, s, C$_5$H$_5$), 3.29 [12 H, s, N(CH$_3$)$_2$], 1.96 (3 H, s, CH$_3$), 1.33 [9 H, s, C(CH$_3$)$_3$] ^{13}C-{^{1}H}:[c] 128.93 (s, C$_6$H$_3$), 123.86 (s, C$_6$H$_3$), 119.94 (s, C$_6$H$_3$), 101.94 (s, C$_5$H$_5$), 73.33 [br, N(CH$_3$)$_2$], 30.95 [s, C(*C*H$_3$)$_3$], 34.99 (s, CH$_3$)
12 [Mo(η-C$_5$H$_5$)(OC$_6$H$_4$Bu^t)(NMe$_2$)$_2$][e] Yellow-orange oil	^{1}H:[c] 7.48 (2 H, d, $J_{\mathrm{HH}} = 7.5$, C$_6$H$_4$), 7.35 (2 H, d, $J_{\mathrm{HH}} = 7.5$, C$_6$H$_4$), 5.68 (5 H, s, C$_5$H$_5$), 2.95 (12 H, s, CH$_3$), 1.33 [9 H, s, C(CH$_3$)$_3$] ^{13}C-{^{1}H}:[c] 123.85 (s, C$_6$H$_4$), 121.71 (s, C$_6$H$_4$), 102.16 (s, C$_5$H$_5$), 85.92 [br, N(CH$_3$)$_2$], 32.66 [s, C(*C*H$_3$)$_3$]
13 [Mo(OC$_6$H$_4$Me-*p*)$_4$(HNMe$_2$)$_2$] Orange crystal C, 62.6 (62.55); H, 6.75 (6.9); N, 4.6 (4.55) FAB mass spectrum: *m/z* 616 (M^+), 526 ($M^+ -$ 2NHMe$_2$) IR (Nujol mull): 3230w [ν(N–H)]	^{1}H:[c] 25.61 (sh), 17.85 (sh), −9.96 (br), −12.56 (br)
14 [Mo(OC$_6$H$_4$Bu^t-*p*)$_4$(HNMe$_2$)$_2$] Orange crystals C, 67.7 (67.5); H, 8.25 (8.5); N, 3.55 (3.6) FAB mass spectrum: *m/z* 738 [Mo(OR)$_4$(NMe$_2$)], 694 [Mo(OR)$_4$], 589 [Mo(OR)$_3$(NMe$_2$)] IR (Nujol mull): 3241w [ν(N–H)]	^{1}H (CD$_2$Cl$_2$): 18.06 (sh), 1.93 (sh), −9.43 (br), −12.98 (br)

[a] Analytical data given as found (calculated) %. All mass spectral data are quoted for ^{98}Mo. Correct isotope patterns were observed. All IR bands are quoted in cm^{-1}. [b] All chemical shifts are quoted in δ and coupling constants in Hz: ^{1}H at 300 MHz, ^{13}C-{^{1}H} at 75.5 MHz. [c] In C$_6$D$_6$. [d] Lower C presumed to arise from loss of traces of solvent after sample weighing. [e] Thermally unstable at r.t.

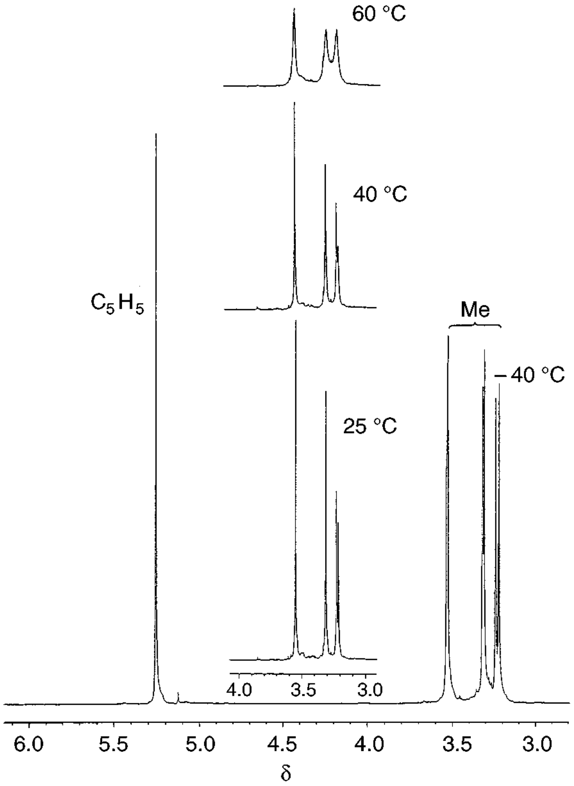

Fig. 3 Variable-temperature 500 MHz ^1H NMR spectra of [Mo(η-C_5H_5)(S_2CNMe_2)$_3$] **5** in $CDCl_3$

Table 3 Selected bond lengths (Å) and angles (°) for compounds **13** and **15**

Compound **13***		Compound **15**	
Mo–O(1)	1.962(3)	Mo–O(1)	1.955(3)
Mo–O(2)	1.964(3)	Mo–O(3)	1.965(3)
Mo–N(1)	2.243(4)	Mo–N(1)	2.220(3)
O(1)–C(1)	1.339(5)	O(1)–C(1)	1.345(4)
O(2)–C(8)	1.374(5)	O(3)–C(15)	1.347(4)
N(1)–C(15)	1.466(6)	N(1)–C(29)	1.403(5)
N(1)–C(16)	1.474(6)	N(1)–C(30)	1.433(5)
N(1)–Mo–N(1′)	180.0	N(1)–Mo–N(2)	174.9(2)
Mo–O(1)–C(1)	145.9(3)	Mo–O(1)–C(1)	140.2(2)
Mo–O(2)–C(8)	131.0(3)	Mo–O(3)–C(15)	134.9(2)

* The values are for molecule **A**; those of molecule **B** are similar.

were slightly more thermally stable and could be isolated, they were too air sensitive for elemental analysis. Their ^1H and ^{13}C NMR chemical shifts are listed in Table 2, compared with those of Bu^{t}OH.

With phenols. Treatment of the compound **1** with the very bulky 2,6-di-*tert*-butyl-4-methylphenol at 60 °C gave a mixture of [Mo(η-C_5H_5)(OC_6H_2Me-4-Bu$^t_2$-2,6)(NMe_2)$_2$] **10** and the starting materials. Compound **10** is thermally stable, but it has a very similar solubility to 2,6-di-*tert*-butyl-4-methylphenol; it was not possible to separate them. The starting compound [Mo(η-C_5H_5)(NMe_2)$_3$] could be removed by sublimation *in vacuo*.

The reaction with the less bulky phenol 2-*tert*-butyl-6-methylphenol (1 equivalent) at room temperature gave [Mo(η-C_5H_5)(OC_6H_3Me-6-Bu^t-2)(NMe_2)$_2$] **11**, which is thermally stable. The ^1H NMR spectrum in C_6D_6 showed **11** to be pure. The two doublets at δ 7.33 and 7.22 and the pseudo-triplet at δ 6.72 are due to the C_6H_3 group, a singlet at δ 5.49 corresponds to the η-C_5H_5 group, the singlet at δ 3.29 is assigned to the NMe_2 groups and a singlet at δ 1.96 corresponds to the Me group on the C_6 ring; finally the singlet at δ 1.33 is due to the Bu^t group. The ^{13}C-{^1H} NMR spectrum is fully consistent with the proposed structure.

Treatment of compound **1** with 1 equivalent of the much less bulky *p*-*tert*-butylphenol (*p*-Bu^tC_6H_4OH) produced a thermally unstable compound [Mo(η-C_5H_5)(OC_6H_4Bu^t-*p*)(NMe_2)$_2$] **12** which decomposed at 20 °C. The structure is tentatively proposed on the basis of the NMR data (Table 2). However, treatment of [Mo(η-C_5H_5)(NMe_2)$_3$] with $\geqslant 3$ equivalents of *p*-Bu^tC_6H_4OH or *p*-cresol (*p*-MeC_6H_4OH) gave the orange crystalline compounds [Mo(OR)$_4$($HNMe_2$)$_2$] (R = *p*-MeC_6H_4 **13** or *p*-Bu^tC_6H_4 **14**). The data show that replacement not only of the amide group but also of the cyclopentadienyl ring has occurred. This is an unusual reaction. Compound **13** has been reported previously by Rothwell and co-workers[7] from the reaction between Mo(NMe_2)$_4$ and *p*-MeC_6H_4OH. The ^1H NMR spectra of **13** and **14** have some very broad peaks and abnormal chemical shifts (see Table 2); ^{13}C NMR spectra could not be obtained. This is consistent with the reported paramagnetism at room temperature of **13**, indeed all octahedral molybdenum(IV) compounds such as [Mo(OR)$_4$($HNMe_2$)$_2$] are paramagnetic.[7] The IR spectra of compounds **13** and **14** show bands at 3230 and 3241 cm^{-1} respectively assignable to the ν(N–H) stretches of the dimethylamine ligand.

An orange crystal of [Mo(OC_6H_4Me-*p*)$_4$($HNMe_2$)$_2$] **13** was mounted in a Lindeman capillary in air and the structure was determined (Fig. 6). Selected bond lengths and angles are given in Table 3. Unexpectedly, the compound was found to be [Mo(OC_6H_4Me)$_4$(NMe_2)$_2$] **15**, formally a molybdenum(VI) compound. It was noted that the crystal was dark purple at the time of data collection. Another orange crystal from the same batch of **13** was mounted but this time under dinitrogen. This crystal contained two crystallographically independent molecules **A** and **B** with similar geometrical parameters (molecule **A** is shown in Fig. 7) in the asymmetric unit and selected distances and angles are given in Table 3. It was found to be the expected compound [Mo(OC_6H_4Me-*p*)$_4$($HNMe_2$)$_2$] **13**. Despite several attempts, it was not possible efficiently to convert **13** into **15** by treatment with dry oxygen.

In both complexes **13** and **15** the ligands adopt an approximately octahedral environment about the metal centre (the angular distortion away from regular octahedral geometry does not exceed 8.1° in **13** and 5.7° in **15**) with the *trans* arrangement of amine ligands [N–Mo–N 180.0° in **13** and 174.9(2)° in **15**]. The molecular structure of **13** closely resembles that of the previously reported [Mo(OC_6H_4Ph-2)$_4$($HNMe_2$)$_2$].[8] Indeed, in **13** the Mo–O [1.959–1.964(3), average 1.961 Å] as well as Mo–N distances [2.243(4) and 2.245(4) Å] are virtually identical to the corresponding values in [Mo(OC_6H_4Ph-2)$_4$($HNMe_2$)$_2$] [Mo–O 1.963(3) and 1.972(3), Mo–N 2.239(4) Å]. In complex **15** the Mo–O distances [1.955–1.973(3), average 1.964 Å] are almost the same as in **13**, whereas the Mo–N distances of 2.220(3) and 2.202(3) Å are somewhat shorter, reflecting the different type of molybdenum–nitrogen bonding in **13** and **15**. The most noteworthy features of the structure of **15** may be associated with the decreasing bulk of the nearly planar NMe_2 group [Σ°(N) 357.4(9) and 355.0(10)°] in comparison with the tetrahedral $HNMe_2$ group in **13**. Thus there is a substantial redistribution of intramolecular contacts between the ligands and this causes significant changes of the mutual orientation of OR substituents. For example, in **13** the opposed benzene rings, due to the centre of symmetry, are *trans* oriented [torsion angles C(1)–O(1)–O(1′)–C(1′) and C(8)–O(2)–O(2′)–C(8′) are 180.0°] and mutually coplanar whereas in **15** they are approximately *cis* oriented [torsion angles C(1)–O(1)–O(3)–C(15) and C(8)–O(2)–O(4)–C(22) are 44.8 and −3.22°] and mutually orthogonal [dihedral angles C(1)–C(6)/C(15)–C(20) and C(8)–C(13)/C(22)–C(27) are 70.2 and 83.8°].

Both compounds **13** and **14** are paramagnetic and the magnetic susceptibility of **14** was determined using the Evans

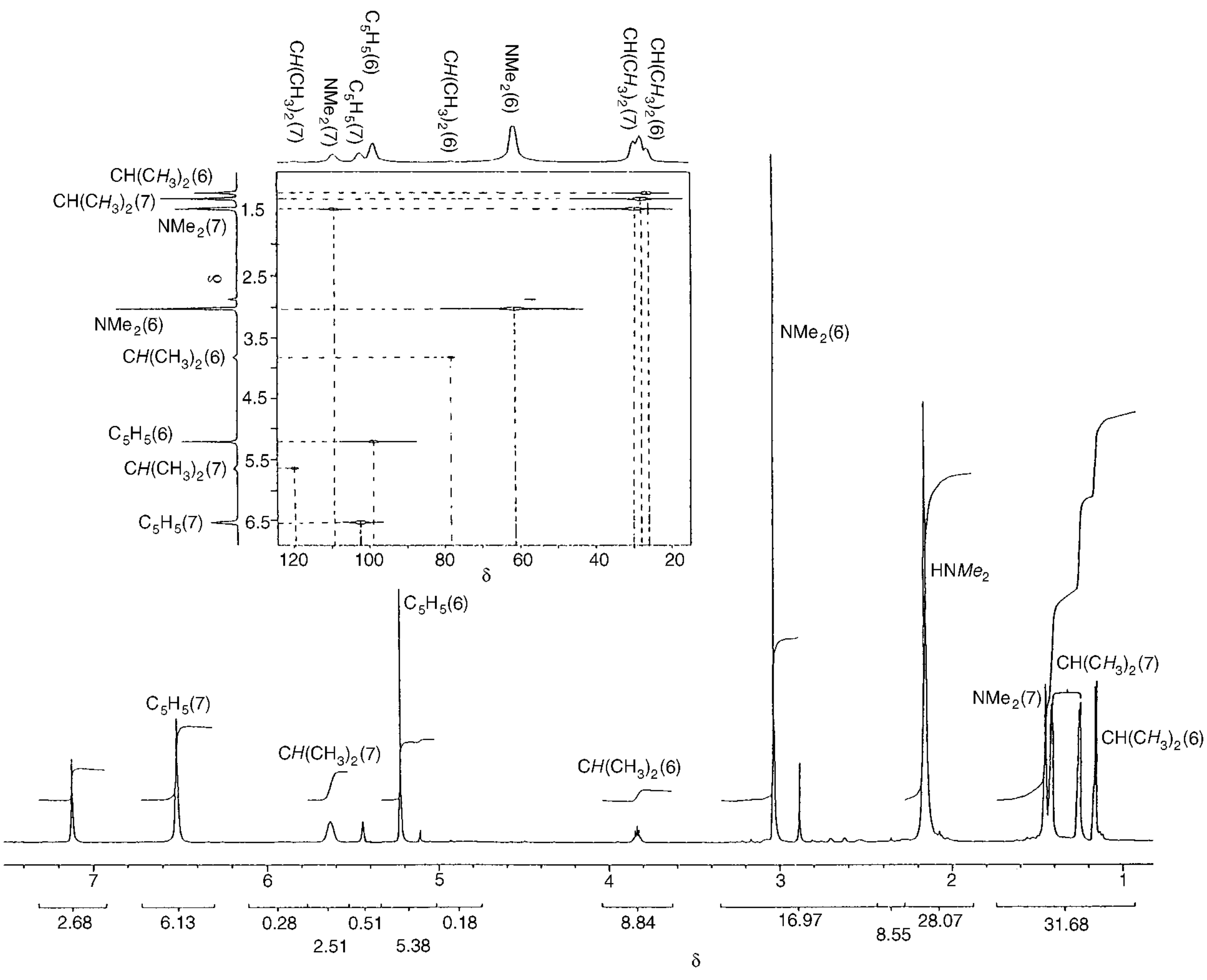

Fig. 4 The 500 MHz ^{1}H and ^{1}H–^{13}C HSQC NMR spectra of [Mo(η-C$_5$H$_5$)(OPr^i)(NMe$_2$)$_2$] **6** and [Mo(η-C$_5$H$_5$)(OPr^i)$_2$(NMe$_2$)] **7** in C$_6$D$_6$ at 25 °C

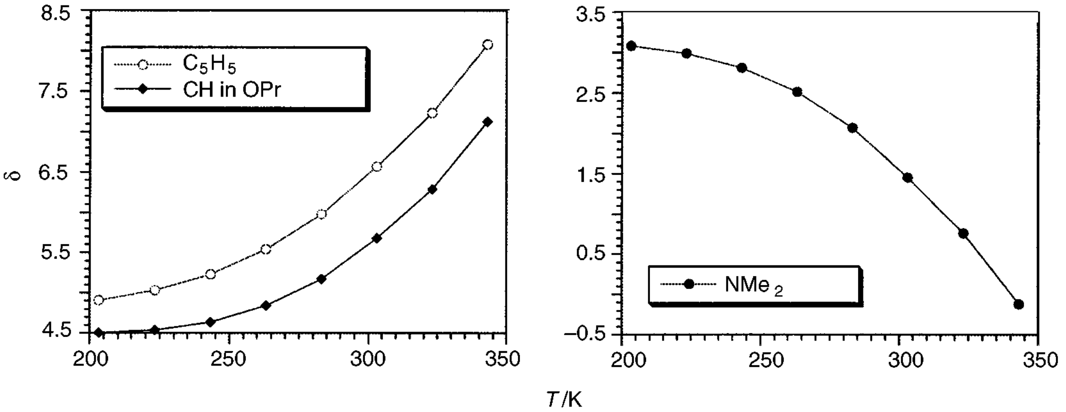

Fig. 5 Dependence of the ^{1}H NMR chemical shifts of compound **7** on temperature

method[24,25] to be μ_{eff} = 2.80 μ_B. This value compares well with the 2.83 μ_B expected for two unpaired electrons, where all the angular momentum is quenched. The paramagnetism of compound **14** is consistent with the point group D_{4h}. Assuming **14** has a similar structure to that of **13**, the crystal structure of **13** shows that the Mo–O bond lengths in the *xy* plane are significantly shorter (1.961 *vs.* 2.244 Å) than the Mo–N bond lengths in the *xz* and *yz* planes, and this may be attributed to a greater degree of σ donation from the aryl oxides compared to the amine. Also some π-donor interactions from the aryl oxides would be expected and both these interactions would lead to the d_{xy} orbital being higher in energy than the d_{xz} and d_{yz} orbitals. Thus the two metal-based electrons in this formally molybdenum(IV) compound would therefore be expected to reside in the degenerate d_{xz} and d_{yz} metal orbitals which are lowest in energy giving rise to **14** being paramagnetic.

Experimental

All preparations and manipulations of air- and/or moisture-sensitive materials were carried out under an atmosphere of dinitrogen or argon, using either standard Schlenk-line techniques or in an inert-atmosphere dry-box containing dinitrogen. Inert gases were purified by passage through columns filled with molecular sieves (4 Å) and either manganese(II) oxide suspended on vermiculite for the vacuum line or BASF catalyst for the

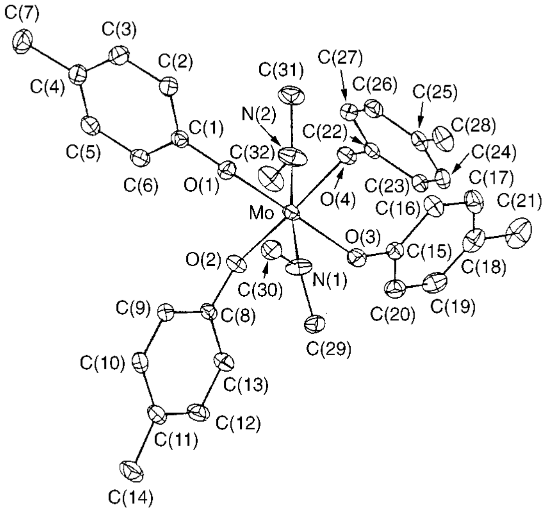

Fig. 6 Molecular structure of [Mo(OC_6H_4Me-*p*)$_4$($HNMe_2$)$_2$] **15**

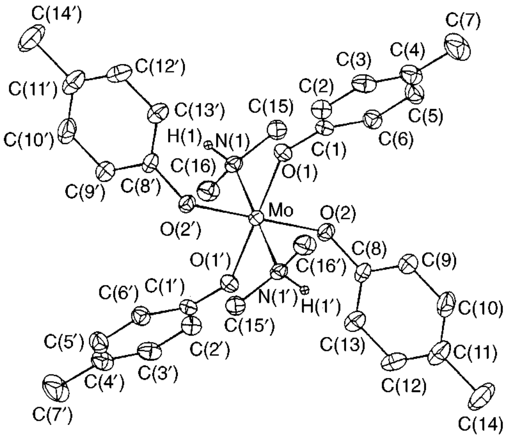

Fig. 7 Molecular structure of [Mo(OC_6H_4Me-*p*)$_4$($HNMe_2$)$_2$] **13**

dry-box. Solvents and solutions were transferred through stainless-steel cannulae, using a positive pressure of inert gas. Filtrations were performed in a similar manner using modified stainless-steel cannulae fitted with glass-fibre filter discs. All glassware and cannulae were thoroughly dried at 150 °C, usually overnight, before use.

All solvents were thoroughly deoxygenated before use either by repeated evacuation followed by admission of dinitrogen, or by bubbling dinitrogen through the solvent for approximately 15 min. Solvents were predried over activated 4 Å molecular sieves and then distilled over sodium (toluene, light petroleum b.p. 100–120 °C), sodium–potassium alloy (diethyl ether, pentane and light petroleum b.p. 40–60 °C), potassium (thf, benzene) or calcium hydride (dichloromethane, acetonitrile) under a mild, continuous stream of dinitrogen. Perdeuteriated solvents for NMR spectroscopy were deoxygenated and dried over calcium hydride (dichloromethane, acetonitrile) or potassium (benzene, thf and toluene) and then distilled before use. Activated alumina (Al_2O_3, neutral, Brockmann I, standard grade, ≈150 mesh) was used for chromatography and deoxygenated before use by repeated evacuation followed by admission of dinitrogen. Celite 545 filtration aid (Koch-Light) was predried at 140 °C and similarly deoxygenated before use.

Nuclear magnetic resonance spectra were recorded on either a Varian UnityPlus 500 (^1H and ^{13}C spectra at 499.868 and 125.704 MHz, respectively) or a Bruker AM300 spectrometer (^1H and ^{13}C at 300.13 and 75.5 MHz, respectively). All two-dimensional experiments were performed using z gradients with an improved version of the pulse sequences (by Dr. P. Sandor, Varian Appl. Lab., Darmstadt, Germany). Indirect detection experiments were carried out on a Varian UnityPlus 500 fitted with a pulsed-field-gradient one-dimensional probe. The spectra were referenced internally using the residual protio solvent (^1H) and solvent (^{13}C) resonances measured relative to $SiMe_4$ (^1H and ^{13}C, δ 0). Mass spectra were recorded on an AEI MS 302 spectrometer, updated by a data-handling system supplied by Mass Spectrometry Services Ltd. Fast atom bombardment (FAB) mass spectra were obtained by the EPSRC Mass Spectrometry Service Centre at the University College of Swansea. The *m/z* values quoted are based on the most abundant isotope of each element. Infrared spectra were recorded on either a Perkin-Elmer 1710 Fourier-transform spectrometer or a Mattson instruments Galaxy series FT-IR 6020 spectrometer in the range 400–4000 cm^{-1} and a Perkin-Elmer 580B spectrometer in the range 200–600 cm^{-1}. Samples were prepared as either Nujol mulls between KBr or NaCl plates, or as KBr or CsI discs. Elemental analyses were obtained by the microanalysis department of the Inorganic Chemistry Laboratory.

Electrochemical studies were performed using an EG & G Princeton Applied Research potentiostat, model 273. The three-electrode configuration consists of a glassy carbon working electrode, platinum-gauze counter electrode and a silver-wire reference electrode. Typically, experiments were carried out in thf (30 cm^3) under dinitrogen at ambient temperature with 0.1 mol dm^{-3} tetrabutylammonium hexafluorophosphate and 1–2 mmol dm^{-3} sample. Potentials were referenced internally or externally to the ferrocenium–ferrocene couple, and reversibility was judged by comparison of ΔE at various scan rates with that of the standard.

Preparations

The compound [Mo(η-C_5H_5)(NMe_2)$_3$] **1** was prepared as previously described.[19]

[Mo(η-$Me_3SiC_5H_4$)(NMe_2)$_3$] 2. The compound Mo(NMe_2)$_4$ (1.25 g, 4.59 mmol) in benzene (30 cm^3) was treated with $Me_3SiC_5H_5$ (2.29 cm^3, 13.77 mmol) at 0 °C. After removal of the ice-bath, the purple solution was stirred at room temperature for 1 d, during which it changed to green. The solvent was removed under reduced pressure and the residue extracted with pentane (3 × 20 cm^3). The pentane was removed and the resulting slightly yellowish green oil dried *in vacuo*. Yield: 1.59 (95%).

[Mo(η-$Me_3SiC_5H_4$)$_2$$H_2$] 3. Trimethylsilylcyclopentadiene (2.44 cm^3, 14.7 mmol) was added to a solution of Mo(NMe_2)$_4$ (1.0 g, 3.67 mmol) in benzene (50 cm^3) and refluxed for 17 h. After this time the solution had changed from purple to brown. The volatiles were removed under reduced pressure. The product was purified by column chromatography on alumina, being eluted with toluene as a yellow-green band.

[Mo(η-C_9H_7)(NMe_2)$_3$] 4. To a solution of Mo(NMe_2)$_4$ (0.125 g, 0.46 mmol) in benzene (25 cm^3), was added indene (0.54 cm^3, 4.6 mmol) at 0 °C. The ice-bath was removed and the purple solution stirred at room temperature for 5 d, changing to yellow-brown. The solvent was removed under reduced pressure and the residue extracted with pentane (3 × 20 cm^3). The volatiles were removed under reduced pressure to afford a yellow-brown oil. Yield: 0.08 g (50%).

[Mo(η-C_5H_5)(S_2CNMe_2)$_3$] 5. Carbon disulfide (2 cm^3) was added dropwise to a frozen solution of Mo(NMe_2)$_4$ (0.4 g, 1.36 mmol) in benzene (20 cm^3) to give a reddish solution. After refluxing for 2 h the solution was filtered through Celite and the residue washed with toluene (200 cm^3). The volume of the solution was reduced to 20 cm^3 and pentane (140 cm^3) was added to precipitate the product as a red-purple powder. The crystalline product was found to contain 0.67 equivalent of toluene, which can be removed by recrystallisation from $CDCl_3$ and pentane. Yield: 0.32 g (45%).

[Mo(η-C_5H_5)(OPr^i)(NMe_2)$_2$] 6. Isopropyl alcohol (0.026 cm^3, 0.34 mmol) was added to a [Mo(η-C_5H_5)(NMe_2)$_3$] (0.10 g, 0.34 mmol) solution in pentane (20 cm^3) at 0 °C and stirred for 30 min. After filtration, removal of the solvent and drying *in vacuo* at 0 °C, [Mo(η-C_5H_5)(OPr^i)(NMe_2)$_2$] was isolated as an air-, moisture- and thermally-sensitive green oil in essentially quantitative yield.

[Mo(η-C_5H_5)(OPr^i)$_2$(NMe_2)] 7. Isopropyl alcohol (0.06 cm^3, 0.78 mmol) was added to a [Mo(η-C_5H_5)(NMe_2)$_3$] (0.10 g, 0.34 mmol) solution in pentane (20 cm^3) at 0 °C and stirred for 30 min. After filtration, removal of the solvent and drying *in vacuo* at 0 °C, [Mo(η-C_5H_5)(OPr^i)$_2$(NMe_2)] was isolated as a very air-, moisture- and thermally-sensitive green oil in essentially quantitative yield.

[Mo(η-C_5H_5)(OBu^t)(NMe_2)$_2$] 8. *tert*-Butyl alcohol (0.03 cm^3, 0.34 mmol) was added to a [Mo(η-C_5H_5)(NMe_2)$_3$] (0.1 g, 0.34 mmol) solution in pentane (20 cm^3) at 0 °C. After removal of the ice-bath, the green solution was stirred at room temperature for 2 h. The product was isolated in almost quantitative yield as a very air- and moisture-sensitive green oil after filtration, removal of the solvent and drying *in vacuo*.

[Mo(η-C_5H_5)(OBu^t)$_2$(NMe_2)] 9. *tert*-Butyl alcohol (0.1 cm^3, 1.0 mmol) was added to a [Mo(η-C_5H_5)(NMe_2)$_3$] (0.10 g, 0.34 mmol) solution in pentane (20 cm^3) at 0 °C. After removal of the ice-bath, the solution was stirred at room temperature overnight. The compound [Mo(η-C_5H_5)(OBu^t)$_2$(NMe_2)] was isolated as a quite air- and moisture-sensitive green oil after filtration, removal of the solvent and drying *in vacuo*. Yield: 0.11 g (95%).

[Mo(η-C_5H_5)(OC_6H_2Me-4-Bu$^t_2$-2,6)(NMe_2)$_2$] 10. To a solution of [Mo(η-C_5H_5)(NMe_2)$_3$] (0.6 g, 2.04 mmol) in pentane (10 cm^3) was added a 2,6-*tert*-butyl-4-methylphenol (0.45 g, 2.04 mmol) solution in pentane (10 cm^3) at room temperature. The reaction was heated to 35 °C for 1 d, with no appreciable colour change. The product was isolated as a green solid, together with the free alcohol, after filtration, removal of the solvent and drying in *vacuo*. No pure product could be obtained.

[Mo(η-C_5H_5)(OC_6H_3Me-6-Bu^t-2)(NMe_2)$_2$] 11. To a solution of [Mo(η-C_5H_5)(NMe_2)$_3$] (0.1 g, 0.34 mmol) in pentane (10 cm^3) was added 2-*tert*-butyl-6-methylphenol (0.056 g, 0.34 mmol) at −78 °C. The reaction was warmed to room temperature and stirred for 2 d. In this time the initially green solution changed to yellow-green. The product was isolated as a greenish brown oil in over 95% yield after filtration, removal of the solvent and drying *in vacuo*.

[Mo(η-C_5H_5)(OC_6H_4Bu^t-*p*)(NMe_2)$_2$] 12. In a glove-box, [Mo(η-C_5H_5)(NMe_2)$_3$] (5.5 mg, 0.019 mmol) was weighed into an NMR tube. A solution of *p*-Bu^tC_6H_4OH (2.7 mg, 0.019 mmol) in C_6D_6 was added. The green solution turned orange-yellow immediately and the ^{1}H NMR spectrum was acquired within 15 min. A solution of *p*-Bu^tC_6H_4OH (0.051 g, 0.34 mmol) in pentane (20 cm^3) was added dropwise to a [Mo(η-C_5H_5)(NMe_2)$_3$] (0.1 g, 0.34 mmol) solution in pentane (15 cm^3) at −78 °C changing to yellow-brown. After rapid filtration the solvent was removed under reduced pressure. The ^{1}H NMR spectrum was identical to that of the *in-situ* preparation.

[Mo(OC_6H_4Me-*p*)$_4$($HNMe_2$)$_2$] 13. The compound [Mo(η-C_5H_5)(NMe_2)$_3$] (0.2 g, 0.68 mmol) in pentane (20 cm^3) was treated dropwise with *p*-MeC_6H_4OH (0.29 cm^3, 2.73 mmol) in pentane (20 cm^3) at −78 °C. The reaction mixture rapidly changed to brown-orange. It was allowed to warm to room temperature slowly and stirred for 1 d. During this time some orange powder formed. The solution was decanted and reduced in volume to 30 cm^3. After cooling to −20 °C more orange powder separated. It was recrystallised twice from pentane at −80 and −20 °C giving orange microcrystals. Yield: 0.19 g (45%).

Table 4 Crystal data, data collection and refinement for compounds **13** and **15**

	13	**15**
Formula	$C_{32}H_{42}MoN_2O_4$	$C_{32}H_{40}MoN_2O_4$
M	614.63	612.62
Crystal size/mm	0.08 × 0.37 × 0.53	0.25 × 0.34 × 0.59
Colour	Orange	Deep purple
Crystal system	Triclinic	Monoclinic
Space group	$P\bar{1}$	$P2_1/c$
a/Å	10.002(1)	18.303(2)
b/Å	13.231(2)	12.183(1)
c/Å	13.326(1)	14.432(2)
α/°	114.89(1)	
β/°	96.166(9)	101.486(9)
γ/°	95.02(1)	
U/Å^3	1573.0(4)	3153.6(6)
Z	2	4
D_c/g cm^{-3}	1.30	1.29
F(000)	644	1280
μ/cm^{-1}	4.40	4.39
T/K	298	298
θ_{max}/°	28	26
Reflections measured	7083	6442
Independent reflections	6650	6179
Total observed data [$I > 3\sigma(I)$]	4113	3587
Merging R	0.021	0.018
Number of parameters	363	352
Data : parameters	11.3 : 1	10.2 : 1
Weighting parameters	7.96, 7.43, 5.00	9.05, −2.09, 6.96
Minimum, maximum residual peaks/e Å^{-3}	−1.04, 0.49	−0.33, 0.46
R	0.046	0.040
R'	0.060	0.043

$R = \Sigma(|F_o| - |F_c|)/\Sigma|F_o|$, $R' = [w\Sigma(|F_o| - |F_c|)^2/\Sigma w|F_o|^2]^{\frac{1}{2}}$.

[Mo(OC_6H_4Bu^t-*p*)$_4$($HNMe_2$)$_2$] 14. A solution of *p*-Bu^tC_6H_4-OH (0.23 g, 1.53 mmol) in pentane (60 cm^3) was added dropwise to a solution of [Mo(η-C_5H_5)(NMe_2)$_3$] (0.15 g, 0.51 mmol) in pentane (15 cm^3) at −78 °C changing immediately from green to red. The reaction mixture was allowed to warm to room temperature and stirred for 12 h. After filtration the volume of the filtrate was reduced to 30 cm^3. Orange microcrystals separated and were recrystallised from pentane at −20 °C. Yield: 0.10 g (25%).

Crystallography

Crystal structure determinations were conducted on an Enraf-Nonius CAD4F diffractometer using graphite-monochromated Mo-Kα radiation (λ = 0.710 69 Å) at room temperature. The general procedure was as follows. A crystal was mounted in a Lindeman tube (0.7 mm) and sealed with a small flame. This was transferred to the goniometer head of an Enraf-Nonius CAD4 diffractometer. Unit-cell parameters were calculated from the setting angles of 24 strong, carefully centred high-angle reflections. Three reflections were chosen as intensity standards and were measured every 3600 s of X-ray exposure time, and three orientation control reflections were measured every 200. The X-ray determination data and experimental details are given in Table 4. A correction for crystal decay (*ca.* 17%) was applied for compound **13**. All data were corrected for Lorentz-polarisation effects and an empirical absorption correction[26] based on azimuthal scan data was applied. Both structures were solved by direct methods. Non-hydrogen atoms were refined with anisotropic thermal parameters by full-matrix least-squares procedures. About 90% of the hydrogen atoms in **13** and 75% in **15** were located in the Fourier-difference maps; the positions of the remainder were calculated. No significant residual electron density was found near the nitrogen atoms of **15**. Attempts to model these nitrogen atoms as four-co-ordinate led to very poor refinements. In **13** the hydrogen atoms attached to the nitrogen atoms were refined isotropically, and the resulting thermal parameters for both nitrogen and hydrogen were consistent with the rest of the structure. In the absence of these hydrogens, refinement was significantly worse, leading to our confidence in the assigned compositions. All hydrogen atoms were included in the final refinement with fixed positional and thermal parameters. A Chebyshev weighting scheme[27] was applied and the data were corrected for the effects of anomalous dispersion. All crystallographic calculations were performed using the CRYSTALS program package on a Micro VAX 3800 computer.[28] Neutral atom scattering factors were taken from the usual sources.[29]

Atomic coordinates, thermal parameters, and bond lengths and angles have been deposited at the Cambridge Crystallographic Data Centre (CCDC). See Instructions for Authors, *J. Chem. Soc.*, *Dalton Trans.*, 1997, Issue 1. Any request to the CCDC for this material should quote the full literature citation and the reference number 186/509.

Acknowledgements

The authors are grateful to Drs. R. Douthwaite, A. Stephens and J. Turner, Professors I. Rothwell and M. Chisholm for helpful discussions. Financial support from Run Run Shaw foundation (student scholarship for X. Y.), BASF AG/Studienstiftung des Deutschen Volkes (post-doctoral fellowship for N. M.) and the EPSRC is also gratefully acknowledged.

References

1 D. C. Bradley and M. H. Chisholm, *J. Chem. Soc. A*, 1971, 2741.
2 M. H. Chisholm, F. A. Cotton and M. W. Extine, *Inorg. Chem.*, 1978, **17**, 1329.
3 M. H. Chisholm, C. E. Hammond and J. C. Huffman, *Polyhedron*, 1988, **7**, 399.
4 M. F. Lappert, P. P. Power, A. R. Sanger and R. C. Srivastava, *Metal and Metalloid Amides: Syntheses, Structures, and Physical and Chemical Properties*, Ellis Horwood, Chichester, 1980.
5 M. H. Chisholm, W. Reichert and P. Thornton, *J. Am. Chem. Soc.*, 1978, **100**, 2744.
6 J. L. Kerschner, J. S. Yu, P. E. Fanwick and I. P. Rothwell, *Organometallics*, 1989, **8**, 1414.
7 S. Beshouri, T. W. Coffindaffer, S. Pirzad and I. P. Rothwell, *Inorg. Chem.*, 1985, **103**, 111.
8 M. J. Bartos, C. E. Kriley, J. S. Yu, J. L. Kerschner, P. E. Fanwick and I. P. Rothwell, *Polyhedron*, 1989, **8**, 1971.
9 D. B. Beach and W. L. Jolly, *Inorg. Chem.*, 1986, **25**, 875.
10 A. K. Hughes, A. Meetsma and J. H. Teuben, *Organometallics*, 1993, **12**, 1936.
11 G. Chandra and M. F. Lappert, *J. Chem. Soc. A*, 1968, 1940.
12 W. A. Herrmann and M. J. A. Morawietz, *J. Organomet. Chem.*, 1994, **482**, 169.
13 W. A. Herrmann, M. J. A. Morawietz and T. Priermeier, *Angew. Chem., Int. Ed. Engl.*, 1994, **33**, 1946.
14 W. A. Herrmann, M. J. A. Morawietz and T. Priermeier, *J. Organomet. Chem.*, 1996, **506**, 351.
15 G. M. Diamond, S. Rodewald and R. F. Jordan, *Organometallics*, 1995, **14**, 5.
16 W. A. Herrmann, M. J. A. Morawietz, H. F. Herrmann and F. Küber, *J. Organomet. Chem.*, 1996, **509**, 115.
17 W. A. Herrmann and W. Baratta, *J. Organomet. Chem.*, 1996, **506**, 357.
18 W. A. Herrmann, W. Baratta and M. J. A. Morawietz, *J. Organomet. Chem.*, 1995, **497**, C4.
19 J. C. Green, R. P. G. Parkin, X. F. Yan, A. Haaland, W. Scherer and M. A. Tafipolsky, unpublished work.
20 T. R. O'Toole, J. N. Younathan, B. P. Sullivan and T. L. Meyer, *Inorg. Chem.*, 1989, **28**, 3923.
21 C. A. McAuliffe and B. J. Sayle, *Inorg. Chim. Acta*, 1978, **30**, 35.
22 D. A. Brown, W. K. Glass and M. A. Burke, *Spectrochim. Acta, Part A*, 1976, **32**, 137.
23 G. B. Deacon, R. S. Dickson, J. L. Latten and B. O. West, *Polyhedron*, 1993, **12**, 497.
24 D. F. Evans, *J. Chem. Soc.*, 1959, 2003.
25 R. A. Bailey, *J. Chem. Educ.*, 1972, **49**, 297.
26 A. C. T. North, D. C. Philips and F. S. Mathews, *Acta Crystallogr., Sect. A*, 1968, **24**, 351.
27 J. S. Rollet, *Computing Methods in Crystallography*, Pergamon, Oxford, 1965.
28 D. J. Watkin, J. R. Carruthers and P. W. Betteridge, *Crystals User Guide*, Chemical Crystallography Laboratory, University of Oxford, 1985.
29 *International Tables for Crystallography*, Kynoch Press, Birmingham, 1974, vol. 4.

Received 17*th February* 1997; *Paper* 7/01096F